Inorg. Chem. **2003**, *42*, 3194–3198

Synthesis, Structure, Electrical Properties, and Band Structure Calculations of TiAsTe

Fu Qiang Huang,[†] Christine Flaschenriem,[†] Paul Brazis,[‡] Carl R. Kannewurf,[‡] and James A Ibers*,[†]

Departments of Chemistry and Electrical and Computer Engineering, Northwestern University, 2145 Sheridan Road, Evanston, Illinois 60208

Received November 25, 2002

The new compound TiAsTe has been synthesized by the reaction of the elements in a LiCl/KCl flux at 923 K. The compound crystallizes with four formula units in space group *Immm* of the orthorhombic system in a cell at 153 K of $a = 3.5730(8)$ Å, $b = 5.249(1)$ Å, $c = 12.794(3)$ Å, $V = 240.0(1)$ Å^3. The structure, which is of the NbPS structure type, is a three-dimensional extended framework built from bicapped $TiAs_4Te_4$ trigonal prisms. It may be considered to comprise $^2_\infty$[TiTe] slabs perpendicular to [001] that are interspersed with linear $^1_\infty$[As] chains running along [010]. The As–As distances alternate at 2.554(2) and 2.695(2) Å. Electrical and thermopower measurements indicate that TiAsTe is an n-type metallic compound. Density functional theory calculations help rationalize the chemical bonding and physical properties.

Introduction

Many group IV and V metal chalcogenides (M/Q) show interesting electronic transport properties.[1−4] Low-dimensional binary chalcogen-rich compounds are associated with the formation of charge density waves (CDWs), which result in an array of unique structural and physical phenomena.[5−11] For example, quasi-one-dimensional $NbSe_3$ exhibits CDW transitions at $T_1 = 145$ K and $T_2 = 59$ K,[7] two-dimensional $ZrTe_3$ exhibits the coexistence of superconductivity and a CDW state,[8,9] and $ZrTe_5$ and $HfTe_5$ exhibit transitions of electronic conductivity and thermopower below 250 K to become potential low-temperature thermoelectric materials.[10] Among simple related ternary chalcogenides NbPS, TaPS, and NbPSe are metallic compounds; NbPS becomes superconducting at 12 K, but NbPSe and TaPS do not superconduct.[12−14]

If a group IV metal atom, such as Ti, were to replace Nb in such a ternary and if the structure were to remain unchanged, then the electric properties of the resultant compound would differ from those of the Nb compound. In fact, the compound $Zr_{3.88}As_{2.79}Te_{5.1}$ [15] adopts the NbPS structure type, with the P site occupied by disordered As and Te atoms. Here we present the synthesis, structure, and some experimental and theoretical physical properties of TiAsTe, which adopts an ordered NbPS structure.

* To whom correspondence should be addressed. E-mail: ibers@chem.northwestern.edu.
† Department of Chemistry.
‡ Department of Electrical and Computer Engineering.

(1) Prodan, A.; Marinkovic, V.; Boswell, F. W.; Bennett, J. C.; Remskar, M. *J. Alloys Compd.* **1995**, *219*, 69−72.
(2) Boswell, F. W.; Bennett, J. C.; Prodan, A. *J. Solid State Chem.* **1999**, *144*, 454−460.
(3) Chaussy, J.; Haen, P.; Lasjaunias, J. C.; Monceau, P.; Waysand, G.; Waintal, A.; Meerschaut, A.; Molinié, P.; Rouxel, J. *Solid State Commun.* **1976**, *20*, 759−763.
(4) Hodeau, J. L.; Marezio, M.; Roucau, C.; Ayroles, R.; Meerschaut, A.; Rouxel, J.; Monceau, P. *J. Phys. C: Solid State Phys.* **1978**, *11*, 4117−4134.
(5) *Electronic Properties of Inorganic Quasi-one-dimensional Compounds*; Monceau, P., Ed.; Physics and Chemistry of Materials with Low-dimensional Structures, Series B: Quasi-One-Dimensional Materials; D. Reidel: Dordrecht, The Netherlands, 1985; parts I and II.
(6) *Crystal Chemistry and Properties of Materials with Quasi-one-dimensional Structures*; Rouxel, J., Ed.; Physics and Chemistry of Materials with Low-Dimensional Structures, Series B: Quasi-One-Dimensional Materials; D. Reidel: Dordrecht, The Netherlands, 1986.
(7) Schäfer, J.; Rotenberg, E.; Kevan, S. D.; Blaha, P.; Claessen, R.; Thorne, R. E. *Physica B* **2002**, *312−313*, 650−652.
(8) Prodan, A.; Marinkovic, V.; Jug, N.; van Midden, H. J. P.; Böhm, H.; Boswell, F. W.; Bennett, J. C. *Surf. Sci.* **2001**, *482−485*, 1368−1373.
(9) Seshadri, R.; Suard, E.; Felser, C.; Finckh, E. W.; Maignan, A.; Tremel, W. *J. Mater. Chem.* **1998**, *8*, 2869−2874.
(10) Felser, C.; Finckh, E. W.; Kleinke, H.; Rocker, F.; Tremel, W. *J. Mater. Chem.* **1998**, *8*, 1787−1798.
(11) Littleton, R. T., IV; Tritt, T. M.; Kolis, J. W.; Ketchum, D. R. *Phys. Rev. B* **1999**, *60*, 13453−13457.
(12) Donohue, P. C.; Bierstedt, P. E. *Inorg. Chem.* **1969**, *8*, 2690−2694.
(13) Shirotani, I.; Kadoya, H.; Sekine, C.; Todo, S.; Yagi, T.; Nakazawa, Y.; Kanoda, K. *J. Phys.: Condens. Matter* **1999**, *11*, 6231−6237.
(14) Keszler, D. A.; Hoffmann, R. *J. Am. Chem. Soc.* **1987**, *109*, 118−124.
(15) Mosset, A.; Jeannin, Y. *J. Less-Common Met.* **1972**, *26*, 285−292.

10.1021/ic020688b CCC: $25.00
Published on Web 04/10/2003

Table 1. Crystal Data and Structure Refinement for TiAsTe

compound	TiAsTe
formula mass	250.42
space group	Immm
a (Å)	3.5730(8)
b (Å)	5.249(1)
c (Å)	12.794(3)
V (Å^3)	240.0(1)
Z	4
T (K)	153(2)
ρ_c (g/cm^3)	6.932
λ (Å)	0.71073
μ (cm^{-1})	287.4
$R(F)^a$	0.0216
$R_w(F_o^2)^b$	0.0605

^{a} $R(F) = \sum||F_o| - |F_c||/|F_o|$ for $F_o^2 > 2\sigma(F_o^2)$. ^{b} $R_w(F_o^2) = \{\sum[w(F_o^2 - F_c^2)^2]/\sum wF_o^4\}^{1/2}$ for all data. $w^{-1} = \sigma^2(F_o^2) + (0.035 \times ((F_o^2 + 2F_c^2)/3)^2$ for $F_o^2 \geq 0$ and $w^{-1} = \sigma^2(F_o^2)$ for $F_o^2 < 0$.

Experimental Section

Synthesis. The following reagents were used as obtained: Ti (Aldrich, 99.5%), As (Alfa, 99.9%), Te (Alfa, 99.9%), LiCl (Aldrich, 99.5%), and KCl (Aldrich, 99.9%). TiAsTe was synthesized by the reaction of 1.0 mmol of Ti, 1.0 mmol of As, and 1.0 mmol of Te, with an additional flux of 200 mg of LiCl/KCl (45/55 by weight). The reaction mixture was loaded into a fused-silica tube under an Ar atmosphere in a glovebox. The tube was sealed under a 10^{-4} Torr atmosphere and then placed in a computer-controlled furnace. The sample was heated to 923 K in 12 h, kept at 923 K for 72 h, and then cooled at 3 K/h to 298 K. The products, which consisted of black shiny needles and some black powder, were washed with water, and then dried with acetone. The needles are TiAsTe, as shown qualitatively by EDX, as performed with an EDX-equipped Hitachi S-4500 SEM, and subsequently shown quantitatively by a crystal-structure determination. The black powder is a mixture of TiAsTe, As, and an unidentified compound containing Ti and Te, as deduced from EDX and an X-ray powder pattern. The yield of needles is over 90%, as deduced from X-ray powder diffraction methods. TiAsTe is stable in air.

Structure Determination. Single-crystal X-ray diffraction data were collected with the use of graphite-monochromatized Mo Kα radiation ($\lambda = 0.71073$ Å) at 153 K on a Bruker Smart-1000 CCD diffractometer.[16] The crystal-to-detector distance was 5.023 cm. Crystal decay was monitored by recollecting 50 initial frames at the end of the data collection. Data were collected by a scan of 0.3° in ω in four groups of 606 frames at ϕ settings of 0°, 90°, 180°, and 270°. The exposure time was 10 s/frame. The collection of the intensity data was carried out with the program SMART.[16] Cell refinement and data reduction were carried out with the use of the program SAINT,[16] and face-indexed absorption corrections were performed numerically with the use of the program XPREP.[17] Then, the program SADABS[16] was employed to make incident beam and decay corrections.

The structure was solved with the direct methods program SHELXS and refined with the full-matrix least-squares program SHELXL of the SHELXTL.PC suite of programs.[17] The final refinement included anisotropic displacement parameters and a secondary extinction correction. Additional experimental details are shown in Table 1. Table 2 gives positional parameters and equivalent isotropic displacement parameters, and Table 3 presents selected bond distances.

Table 2. Atomic Coordinates and Equivalent Isotropic Displacement Parameters for TiAsTe

atom	x	y	z	U_{eq} (Å^2)
Ti	$^1/_2$	0	0.11847(9)	0.0054(4)
As	0	0.2567(1)	0	0.0056(3)
Te	0	0	0.29073(3)	0.0056(3)

Table 3. Bond Distances (Å) for TiAsTe

bond	distance
Ti−As × 4	2.703(1)
Ti−Te × 2	2.837(1)
Ti−Te × 2	2.870(1)
As−As	2.554(2)
As−As	2.695(2)

Electrical Conductivity. The composition TiAsTe of two single crystals was confirmed with EDX measurements. The electrical conductivity of the single-crystal samples was measured with the use of a computer-controlled four-probe technique.[18] Electrical contacts consisted of fine gold wire (25 and 60 μm diameter) attached to the crystals with gold paste. Samples were placed under vacuum for at least 24 h to allow the gold paste to dry completely, which improved contact performance. Excitation currents were kept as low as possible, typically below 1 mA, in order to minimize any nonohmic voltage response and thermoelectric effects at the contact−sample interface. Measurements of the sample cross-sectional area and voltage probe separation were made with a calibrated binocular microscope.

Thermopower Measurements. Variable-temperature thermopower data were taken with the use of a computer-controlled slow-ac measurement technique.[19] The measurement apparatus featured Au-(0.07% Fe)/Chromel differential thermocouples for monitoring the applied temperature gradients. Samples were mounted on 60 μm gold wire by means of gold paste. Fine gold wire (10 μm in diameter) was used for sample voltage contacts, which were made as long as possible in order to minimize thermal conduction through the leads. The sample and thermocouple voltages were measured with the use of Keithley model 181 and Keithley model 182 nanovoltmeters, respectively. The applied temperature gradient was in the range 0.1−0.4 K. Measurements were taken under a turbopumped vacuum maintained below 10^{-5} Torr. The sample chamber was evacuated for 1−3 h prior to cooling to remove any residual water vapor or solvents in the gold paste.

TB-LMTO Calculations. The electronic structure of TiASTe was calculated by means of the self-consistent, scalar relativistic linearized muffin-tin orbital program of Andersen et al.[20−22] within the atomic sphere approximation (ASA). This method splits the crystal space into overlapping atomic spheres (Wigner−Seitz spheres) whose radii are chosen to fill completely the crystal volume. The atomic radii were 3.01, 2.80, and 3.20 bohr for Ti, As, and Te, respectively, and the radii of the three empty spheres were 2.03, 1.59, and 1.25 bohr for E, E1, and E2, respectively. In the calculations presented here, the von Barth−Hedin exchange-correction potential was used within the local density approximation (LDA).[23] All k-space integrations were performed with the tetra-

(16) *SMART Version 5.054 Data Collection and SAINT-Plus Version 6.22 Data Processing Software for the SMART System*; Bruker Analytical X-ray Instruments, Inc.: Madison, WI, 2000.
(17) Sheldrick, G. M. *SHELXTL DOS/Windows/NT Version 6.12*; Bruker Analytical X-ray Instruments, Inc.: Madison, WI, 2000.
(18) Lyding, J. W.; Marcy, H. O.; Marks, T. J.; Kannewurf, C. R. *IEEE Trans. 1nstrum. Meas.* **1988**, *37*, 76−80.
(19) Marcy, H. O.; Marks, T. J.; Kannewurf, C. R. *IEEE Trans. Instrum. Meas.* **1990**, *39*, 756−760.
(20) Andersen, O. K. *Phys. Rev. B* **1975**, *12*, 3060−3083.
(21) Andersen, O. K.; Jepsen, O. *Phys. Rev. Lett.* **1984**, *53*, 2571−2574.
(22) Jepsen, O.; Andersen, O. K. *Z. Phys. B: Condens. Matter* **1995**, *97*, 35−47.
(23) Hedin, L.; Lundqvist, B. I. *J. Phys. Chem. Solids* **1971**, *4*, 2064−2083.

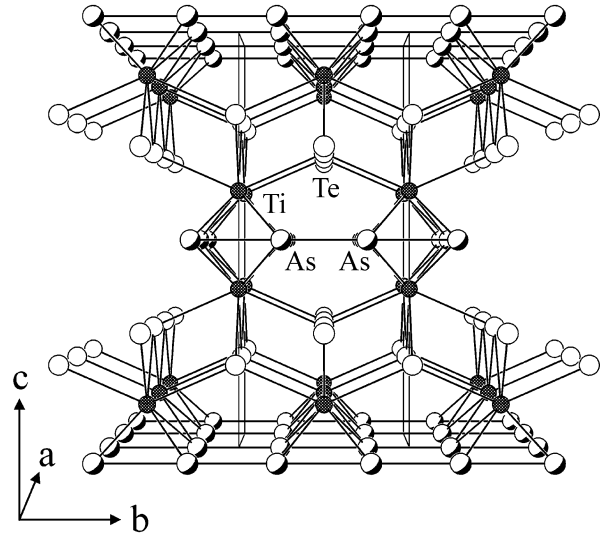

Figure 1. Unit cell of TiAsTe viewed down [100].

hedron method.[24,25] The basis sets consisted of the valence 3d, 4s, and 4p for Ti; 4s and 4p for As; 5s and 5p for Te; and 1s for empty spheres (E, E_1, and E_2). The 4d for As, 4f and 5d for Te, and p−d states for empty spheres were downfolded by the means of Löwdin's technique.[26] The crystal orbital Hamiltonian population (COHP),[27] which is the density of states weighted by the corresponding Hamiltonian matrix element, was calculated to analyze the strength and nature of the bonding. Within the Brillouin zone based on the primitive cell of TiAsTe, 4505 irreducible *k* points were used. The high-symmetry points are Γ (0, 0, 0), X ($^1/_2$, $^1/_2$, $-^1/_2$), W($^3/_4$, $-^1/_4$, $-^1/_4$), R($^1/_2$, 0, 0), S($^1/_2$, 0, $^1/_2$), and T($^1/_2$, 0, $-^1/_2$) in terms of the reciprocal basis vectors.[28]

Results

Synthesis. The compound TiAsTe has been synthesized from the elements in a LiCl/KCl flux at 923 K in greater than 90% yield.

Crystal Structure. TiAsTe adopts the NbPS structure type, with Ti, As, and Te substituting for the positions of Nb, P, and S in NbPS, respectively. The crystal structure of TiAsTe is illustrated in Figure 1. It comprises $^2_\infty$[TiTe] slabs perpendicular to [001] that are interspersed with linear $^1_\infty$[As] chains running along [010]. The three-dimensional framework results from Ti−As bonds. In the structure, the Ti, As, and Te atoms are at sites of *mm*2, *m*2*m*, and *mm*2 symmetry, respectively. The Ti atom is coordinated to a bicapped trigonal prism of four As atoms and four Te atoms, with Te atoms at the capping positions (Figure 2a). Each Te atom is tetrahedrally coordinated to four Ti atoms, and each As atom is coordinated to four Ti and two neighboring As atoms in the same chain, as shown in Figures 1 and 2b. The Ti−As bond distance of 2.703(1) Å (Table 3) is in the range

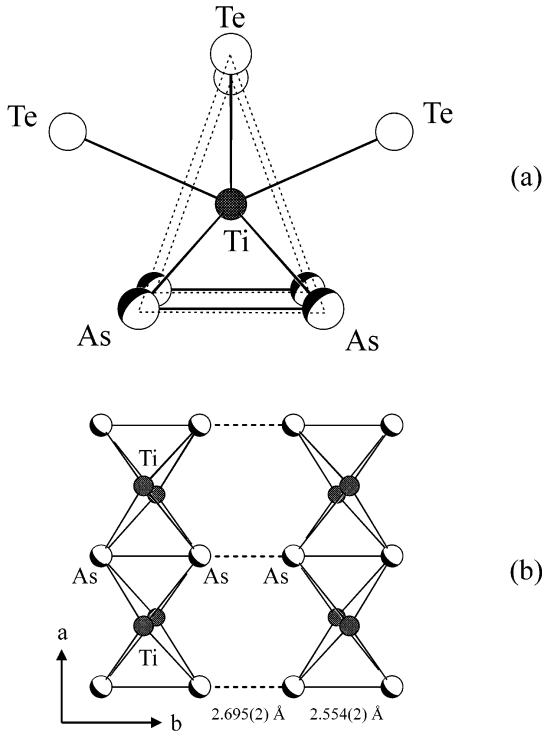

Figure 2. (a) $TiAs_4Te_4$ bicapped trigonal prism and (b) the fragment of the $^2_\infty$[TiAs] slab on (001).

of those found in $TiAs_2$ (2.61(2)−3.06(2) Å),[29] and the Ti−Te bond distances of 2.837(1) and 2.870(1) Å are in the range of those in $Cs_3Ti_3Te_{11}$ (2.716−2.883 Å).[30]

Figure 2b also displays the As chains. Each chain has two different As−As bond distances, 2.554(2) Å (—) and 2.695(2) Å (- - -). The single bond distance in elemental As is 2.516(1) Å.[31] In LnAsTe (Ln = rare-earth element), there is a zigzag As chain, with the unique As−As distance[32] ranging from 2.6350(9) Å in LaAsTe to 2.5915(5) Å in ErAsTe. Given that there are no Te···Te distances within bonding range in TiAsTe, the formal oxidation state of Te is −2. If the oxidation state of Ti is +3 ($3d^1$ electronic configuration), then the linear As^{1-} chain should comprise only As−As single bonds. If the oxidation state of Ti is +4 ($3d^0$ electronic configuration), then the linear As^{2-} chain in the extreme would consist of separated As_2^{2-} dimers with no interaction between dimers. In fact, the short As−As bond 2.554(2) Å in length in TiAsTe is of single-bond length, but the longer As−As bond 2.695(2) Å in length is slightly longer than a single-bond length but definitely short enough for a bonding interaction. Hence, the formal oxidation states may be taken as intermediate, namely $3 + \delta$ for Ti and $-(1 + \delta)$ for As, where $0 < \delta < 1$. Formal oxidation states and bonding in electron-rich polyanionic networks have been discussed in detail recently.[33]

(24) Lambrecht, W. R. L.; Andersen, O. K. *Phys. Rev. B* **1986**, *34*, 2439−2449.
(25) Jepsen, O.; Andersen, O. K. *Solid State Commun.* **1971**, *9*, 1763−1767.
(26) Löwdin, P.-O. *J. Chem. Phys.* **1951**, *19*, 1396−1401.
(27) Dronskowski, R.; Blöchl, P. E. *J. Phys. Chem.* **1993**, *97*, 8617−8624.
(28) Bradley, C. J.; Cracknell, A. P. *The Mathematical Theory of Symmetry in Solids. Representation theory for point groups and space groups*; Clarendon Press: Oxford, 1972.
(29) Wenglowski, S.; Bokii, G. B.; Pobedimskaya, E. A. *J. Struct. Chem. (Engl. Trans.)* **1964**, *5*, 55−59.
(30) Pell, M. A.; Ibers, J. A. *Chem. Mater.* **1996**, *8*, 1386-1390.
(31) Wells, A. F. *Structural Inorganic Chemistry*, 5th ed.; Clarendon Press: Oxford, 1984.
(32) Huang, F. Q.; Brazis, P.; Kannewurf, C. R.; Ibers, J. A. *Inorg. Chem.* **2000**, *39*, 3176−3180.
(33) Papoian, G. A.; Hoffmann, R. *Angew. Chem., Int. Ed.* **2000**, *39*, 2408−2448.

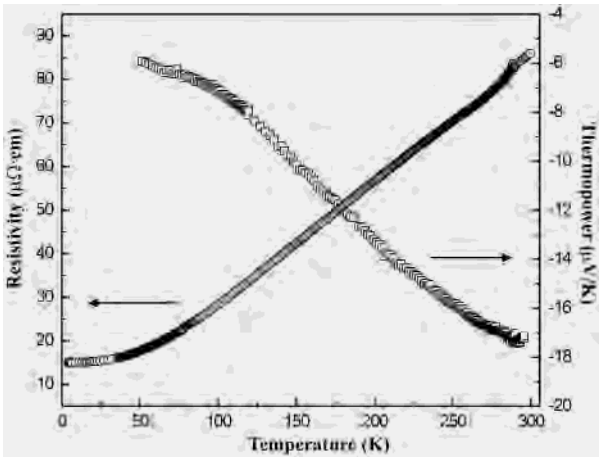

Figure 3. Electrical resistivity and thermopower vs temperature for TiAsTe.

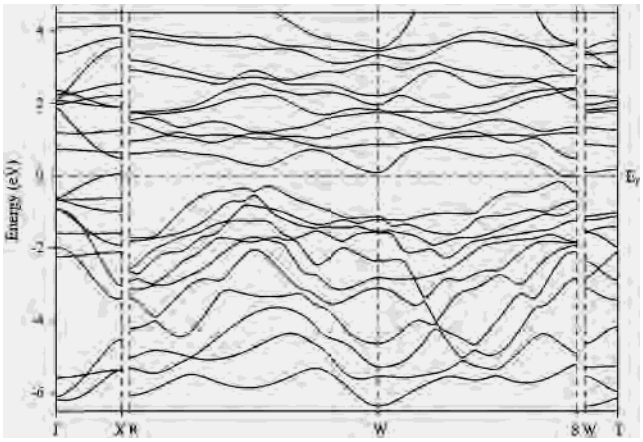

Figure 4. Band structure of TiAsTe, where Γ (0, 0, 0), X ($^1/_2$, $^1/_2$, $-^1/_2$), W($^3/_4$, $-^1/_4$, $-^1/_4$), R($^1/_2$, 0, 0), S($^1/_2$, 0, $^1/_2$), and T($^1/_2$, 0, $-^1/_2$) are the special *k*-points.

Among binary compounds, only UTe_2 [34] possesses the NbPS structure type; U occupies the Ti position, Te(1) occupies the Te position, and Te(2) occupies the As position when compared with the present TiAsTe structure. The Te(2)−Te(2) distances are 3.057(1) and 3.076(1) Å. The oxidation states for U, Te(1), and Te(2) have been assigned as $4 - \delta$, -2, $-(2 - \delta)$, respectively, where $0 < \delta < 1$.[35]

Electrical Conductivity and Thermopower. Figure 3 shows the resistivity and the thermopower of TiAsTe along the needle (*a*) axis as a function of temperature. The material exhibits metallic behavior in that direction. The decline of the resistivity of TiAsTe with decreasing temperature is nearly linear from 300 to 50 K. The thermopower increases from about -17 to -5 μV/K as the temperature decreases from 300 to 50 K; this behavior is characteristic of an n-type metal.

DFT Calculations. The band structure of TiAsTe is displayed in Figure 4. All the bands are distributed either right below or right above the Fermi surface, and none cross it. The highest occupied molecular orbital (HOMO) is at X

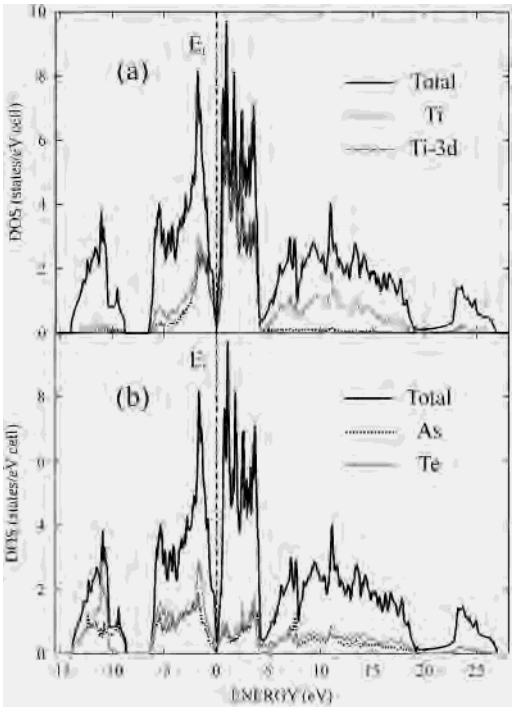

Figure 5. Total density of states (DOS) of TiAsTe and the partial DOS for (a) Ti and Ti-3d and (b) As and Te.

($^1/_2$, $^1/_2$, $-^1/_2$), and the lowest unoccupied molecular orbitals (LUMOs) near S ($^1/_2$, 0, $^1/_2$) are also on the Fermi surface. The indirect band gap of TiAsTe is 0, and the direct band gap near S is about 0.015 eV; excitation of electrons from the valence bands to the conduction bands should be very facile. From these calculations, it follows that TiAsTe should be a metal or a semimetal. The metallic behavior found experimentally could well arise from imperfections and distortions in the crystal structure. NbPQ (Q = S, Se) has a similar band structure, but it is a metal because the additional valence electron contributed from each Nb atom lifts the Fermi level up to cross the Nb-4d bands.

Figure 5 shows the total and partial density of states (DOS) of TiAsTe. The Ti-4s and Ti-4p orbitals are unoccupied and are located from about 4 to 20 eV. Many occupied states from As-4p and Te-5p are in the range -6 to 0 eV, and some states involved in Ti−As and Ti−Te antibonding are in the range 0−4 eV. The DOS from about -14 to -8 eV consists of As-4s and Te-4s. The DOS of Ti-3d mainly distributes around the Fermi level. The Ti-3d states are broken into two parts at the Fermi level, and the five Ti-3d orbitals are degenerate. The DOS of As are also split into two parts at the Fermi level, as a result of the alternating distances in the linear As chain. There are many electronic states between -6 and 4 eV, but there is a deep drop at the Fermi level, where the value is about 0.36 states/eV cell. The partial DOS of Ti, Ti-3d, As, and Te also display this drop, consistent with no bands crossing the Fermi level.

The overall shapes of total and partial DOS of NbPS are similar to those in TiAsTe. One more valence electron from each Nb atom raises the Fermi level right through one peak dominated by Nb-4d orbitals, and the large amount of DOS

(34) Haneveld, A. J. K.; Jellinek, F. *J. Less-Common Met.* **1970**, *21*, 45−49.
(35) Huang, F. Q.; Ibers, J. A. *J. Solid State Chem.* **2001**, *159*, 186−190.

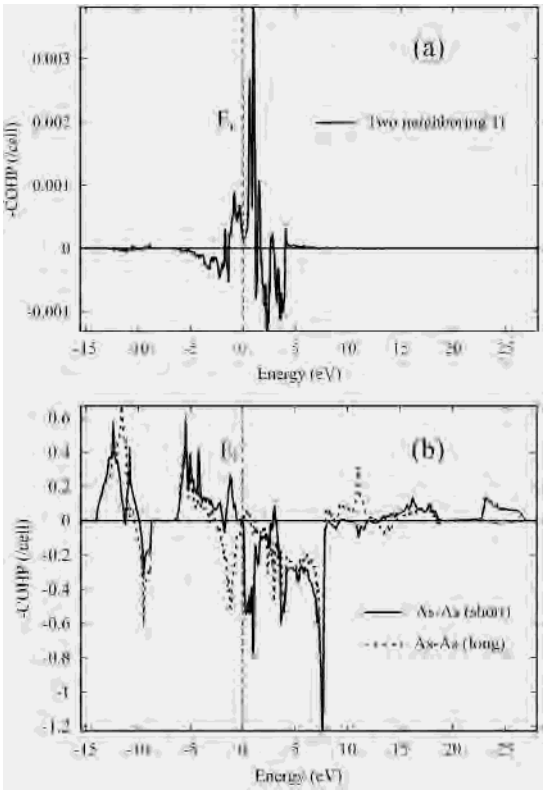

Figure 6. Crystal orbital Hamiltonian populations (−COHPs) (a) between two neighboring Ti atoms, and (b) between the short As−As bond (2.554(2) Å) and between the long As−As bond (2.695(2) Å). (Negative, zero, and positive values of −COHP represent antibonding, nonbonding, and bonding, and the absolute value indicates the bonding strength.)

at the peak is related to a high T_c in NbPS. The Fermi level in NbPSe is not through a DOS peak, and NbPSe is not a superconductor.[14]

A better understanding of the bonding in TiAsTe may be obtained from the crystal orbital Hamiltonian populations (COHPs).[27] The plots of −COHP versus energy for two Ti atoms and two sets of two As atoms are displayed in Figure 6. The −COHP of two Ti atoms is very small. Integration of the −COHP up to the Fermi level gives essentially zero, and hence there is no bonding between the two Ti atoms. The values of the −COHPs between two sets of two As atoms are large. The interaction between the two As atoms separated by 2.554(2) Å changes from bonding to nonbonding as the energy level increases to the Fermi level. Each As atom donates one electron to form this As−As single bond, consistent with experiment. The −COHP values for the other set of two As atoms separated by 2.695(2) Å are negative just below the Fermi level. Although the interaction of these As atoms contains some portion of antibonding energy levels, the overall interaction is still bonding. Thus, these calculations indicate that each As atom donates more than one electron but less than two electrons to form the bond; hence, the oxidation states for Ti, As, and Te should be $3 + \delta$, $-(1 + \delta)$, and -2, respectively, where $0 < \delta < 1$.

Acknowledgment. This research was supported by National Science Foundation Grant DMR00-96676. Use was made of the Central Facilities supported by the MRSEC program of the National Science Foundation (Grant DMR00-76097) at the Materials Research Center of Northwestern University.

Supporting Information Available: Crystallographic file in CIF format for TiAsTe. This material is available free of charge via the Internet at http://pubs.acs.org.

IC020688B